

Military Technical College
Kobry El-Kobbah,
Cairo, Egypt.



13th International Conference
on Applied Mechanics and
Mechanical Engineering.

WRINKLING PREDICTION FOR MIXED-HARDENING METALS IN DEEP-DRAWING PROCESS

WIRATKASEM* K. and HARNCHOOWONG** S.

ABSTRACT

Wrinkling in deep-drawing process was analyzed as the form of short-wavelength shallow buckling modes based on the Donnell-Mushtari-Vlasov shell theory. The local analysis considered the current deformed state of a sheet element in a doubly-curved, biaxial plane stress state. The yield criterion for mixed-hardening metal used J2 yield criterion for isotropic metal and Hosford's yield criterion for anisotropic metal. The effect of back stresses on wrinkling limit curves was investigated numerically.

KEY WORDS: Wrinkling, Mixed-hardening, Bifurcation

NOMENCLATURE

| | |
|-------------------------------------|---|
| $\dot{E}_{\alpha\beta}$ | the incremental stretching strain |
| $\dot{K}_{\alpha\beta}$ | the incremental bending strain |
| $\dot{N}^{\alpha\beta}$ | the incremental stress resultants at buckling |
| $\dot{M}^{\alpha\beta}$ | the incremental bending moments at buckling |
| \dot{U}_{α} | the incremental displacements in the surface-coordinate directions (X_1, X_2) |
| \dot{W} | the incremental buckling displacement normal to the middle surface of the sheet |
| $\dot{\sigma}^{\alpha\beta}$ | the stress rates |
| $\dot{\epsilon}_{\alpha\beta}$ | the strain rates |
| $\bar{L}^{\alpha\beta\kappa\gamma}$ | the plane-stress incremental moduli |
| θ | the angle at which the wrinkles form with respect to the X_1 axis |
| λ | a non-dimensional wave number |
| S | the region of the sheet middle surface over which the wrinkles occur |
| L | the wavelength of the wrinkles |

* Graduate student, Dpt. of Mechanical Engineering, King Mongkut's University of Technology North Bangkok, Bangkok, Thailand.

** Professor, Dpt. of Mechanical Engineering, King Mongkut's University of Technology North Bangkok, Bangkok, Thailand.

INTRODUCTION

Wrinkling is one of defects in sheet metal forming operations. It is produced by a compressive stress field. The prediction of wrinkling is important for the design of stamping and deep-drawing processes. A large number of wrinkling analyses are based on the functional and bifurcation criterion proposed by Hutchinson [1] in his theory of plastic buckling. The criterion was applied by Hutchinson and Neale [2] in a local wrinkling analysis for doubly curved sheet under the biaxial plane stress state. Neale and Tugcu [3] proposed the concept of the wrinkling limit curves for plastic yielding, J2-flow and J2-deformation theory. Kim and Son [4] presented the wrinkling limit curves for the metals with anisotropy described by the yield criteria proposed by Hosford [5]. Tugcu et al. [6] presented the wrinkling limit curves for the metals with planar anisotropy described by two anisotropic yield criteria proposed by Barlat et al.[7] and Karafillis and Boyce [8]. Correia and Ferron [9,10,11] presented the wrinkling limit curves and wrinkling limit curves in deep-drawing process for the metals with planar anisotropy described by yield criteria proposed by Ferron [12].

This study extends the work of Neale and Tugcu [3] by considering the effect of back stress on the critical conditions of wrinkling formation. A numerical analysis of wrinkling limit curves for mixed hardening metals in deep-drawing process is presented.

PROBLEM FORMULATION AND ANALYSIS

In this study, the wrinkle is considered as a plastic bifurcation phenomenon in a sheet metal forming operation. It is often confined to a localized region of the sheet. The buckling mode is thus a local mode, which depends on the local curvatures, the thickness of the sheet, its material properties, and the local stress state, as shown in Fig.1. Here the principal radii of curvature R_1 , R_2 and the sheet thickness t are assumed to be constant. Furthermore, the stress state prior to wrinkling (σ_1, σ_2, τ) is assumed to be a uniform membrane state over the local element being examined for susceptibility to wrinkling.

The short-wavelength wrinkling modes are shallow and can be analyzed using the Donnell-Mushtari-Vlasov (DMV) shallow shell theory [1]. Moreover, this theory restricts the analysis to modes for which the characteristic wavelength of the buckles is large compared to the sheet thickness, yet small compared to the local radii of curvature (R_1, R_2)

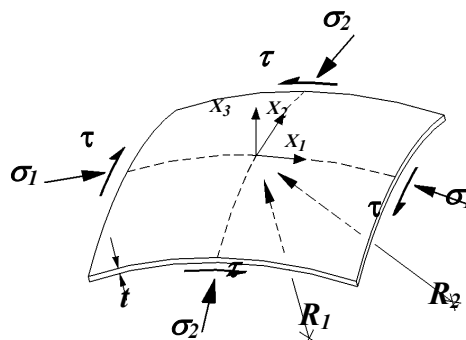


Fig. 1. The geometry and loading of a doubly curved sheet.

According to the DMV theory the buckling mode generates incremental stretching strain ($\dot{E}_{\alpha\beta}$) and bending strain ($\dot{K}_{\alpha\beta}$) in the sheet element. These are given by:

$$\begin{aligned}\dot{E}_{\alpha\beta} &= \frac{1}{2}(\dot{U}_{\alpha,\beta} + \dot{U}_{\beta,\alpha}) + b_{\alpha\beta}\dot{W} + \frac{1}{2}\dot{W}_{,\alpha}\dot{W}_{,\beta} \\ \dot{K}_{\alpha\beta} &= -\dot{W}_{,\alpha\beta}\end{aligned}\tag{1}$$

where the range of Greek indices is 1-2 and a comma denotes covariant differentiation with respect to the surface coordinates. \dot{U}_{α} are the incremental displacements in the surface-coordinate directions (X_1, X_2), \dot{W} is the incremental buckling displacement normal to the middle surface of the sheet, and $b_{\alpha\beta}$ is the curvature tensor of the middle surface in the prebuckling state. The above incremental strains lead to incremental stress resultants ($\dot{N}^{\alpha\beta}$) and bending moments ($\dot{M}^{\alpha\beta}$) at buckling. These are given by

$$\begin{aligned}\dot{N}^{\alpha\beta} &= t\bar{L}^{\alpha\beta\kappa\gamma}\dot{E}_{\kappa\gamma} \\ \dot{M}^{\alpha\beta} &= \frac{t^3}{12}\bar{L}^{\alpha\beta\kappa\gamma}\dot{K}_{\kappa\gamma}\end{aligned}\tag{2}$$

where $\bar{L}^{\alpha\beta\kappa\gamma}$ are the plane-stress incremental moduli relating stress rates $\dot{\sigma}^{\alpha\beta}$ to strain rates $\dot{\epsilon}_{\alpha\beta}$ through

$$\dot{\sigma}^{\alpha\beta} = \bar{L}^{\alpha\beta\kappa\gamma}\dot{\epsilon}_{\kappa\gamma}\tag{3}$$

The critical stress state at buckling is determined by using the following Hutchinson's "bifurcation functional" :

$$F(\dot{U}_{\alpha}, \dot{W}) = \int_S [\dot{M}^{\alpha\beta}\dot{K}_{\alpha\beta} + \dot{N}^{\alpha\beta}\dot{E}_{\alpha\beta} + N^{\alpha\beta}\dot{W}_{,\alpha}\dot{W}_{,\beta}]dS\tag{4}$$

where S is the region of the sheet middle surface over which the wrinkles occur. The condition that $F > 0$ for all admissible fields $\dot{U}_{\alpha}, \dot{W}$ ensures that bifurcation will not occur. Conversely, buckling first becomes possible when $F = 0$ for some non-zero field. The velocity field giving the short wavelength wrinkling mode of the form shown in Fig 2. These are given by

$$\begin{aligned}
 \dot{W} &= At \cos \left[\frac{\lambda}{l} (X_1 \cos \theta + X_2 \sin \theta) \right] \\
 \dot{U}_1 &= Bt \sin \left[\frac{\lambda}{l} (X_1 \cos \theta + X_2 \sin \theta) \right] \\
 \dot{U}_2 &= Ct \sin \left[\frac{\lambda}{l} (X_1 \cos \theta + X_2 \sin \theta) \right]
 \end{aligned} \tag{5}$$

where $l = \sqrt{Rt}$ and R is identified with either R_1 or R_2 , as appropriate. A , B and C are constants representing the relative displacement amplitudes of the mode shape, θ denotes the angle at which the wrinkles form with respect to the X_1 axis, and λ is a non-dimensional wave number. The wavelength of the wrinkles in Fig. 2 is given by $L = 2\pi / \lambda$.

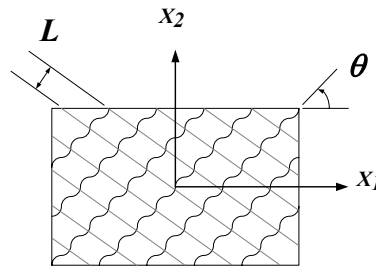


Fig. 2. The Short-wavelength wrinkling mode for sheet element.

In employing the fields (5) we anticipate that wrinkling occur over a certain region S of the sheet which spans many wavelengths of the buckling mode. The boundary conditions or continuity conditions along the edges of S then become relatively unimportant.

The analysis involves substituting the velocity fields (5), the incremental stretching strain and bending strain (1) and the incremental stress resultants and bending moments (2) into the bifurcation functional (4) and integrating over S . We also define $b_{11} = 1/R_1$, $b_{22} = 1/R_2$, as well as $N^{11} = -t\sigma_1$, $N^{22} = -t\sigma_2$ and $N^{12} = -t\tau$ where σ_1 , σ_2 and τ are the current membrane stresses with respect to the geometric axes. The following formulas are also used.

$$\begin{aligned}
 \int_S \sin^2 \left[\frac{\lambda}{l} (X_1 \cos \theta + X_2 \sin \theta) \right] dS &= \frac{S}{2} \\
 \int_S \cos^2 \left[\frac{\lambda}{l} (X_1 \cos \theta + X_2 \sin \theta) \right] dS &= \frac{S}{2}
 \end{aligned} \tag{6}$$

The functional (4) can then be written as

$$F = \frac{1}{2} S t \left(\frac{t}{l} \right)^2 \mathbf{u}^T \mathbf{M} \mathbf{u} \quad (7)$$

where $\mathbf{u} = (A, B, C)$ is the buckling displacement-amplitude vector. The components of the matrix \mathbf{M} as well as the numerical solution routine is given by Neale and Tugcu [3]. The incremental moduli $\bar{\mathbf{L}}$ depend on the particular constitutive law employed.

The buckling in the mode (5) is possible when the associated bifurcation functional $F = 0$. In view of (7), this first occurs when the determinant of \mathbf{M} vanished. To determine the critical stress values σ_1^{cr} , σ_2^{cr} , τ^{cr} for which short-wavelength buckling first occurs, we minimize this determinant with respect to the waveform parameters λ and θ (or equivalently λ_1 and λ_2) and set the minimum equal to zero. The obtained values of λ and θ describe the corresponding critical wrinkling pattern. Therefore, the three equations are solved simultaneously :

$$\begin{aligned} D = \det \mathbf{M} &= 0, \\ \frac{\partial D}{\partial \lambda} = \frac{\partial D}{\partial \theta} &= 0 \end{aligned} \quad (8)$$

We use the Newton-Raphson technique for solving the critical stress values.

CONSTITUTIVE LAWS

In order to clarify the effect of back stress for mixed-hardening metals on the wrinkling initiation, J2 yield criterion with mixed-hardening and Hosford yield criterion with mixed-hardening are adopted.

J2 yield criterion with mixed-hardening is adopted for isotropic metal sheets, given by

$$f = \sigma_e = \left[\frac{3}{2} (S_{ij} - g_{ij})(S_{ij} - g_{ij}) \right]^{\frac{1}{2}} \quad (9)$$

where σ_e is the effective stress, S_{ij} is the deviatoric stress and g_{ij} is the deviatoric part of the back stress.

Hosford's yield criterion with mixed-hardening is adopted for anisotropic metal sheet, given by

$$f = \sigma_e = \left[\frac{1}{(1+\bar{R})} \left\{ \omega_1^m + \omega_2^m + \bar{R} \omega_3^m \right\} \right]^{\frac{1}{m}} \quad (10)$$

where m is known as six for bcc metals and eight for fcc metals, and

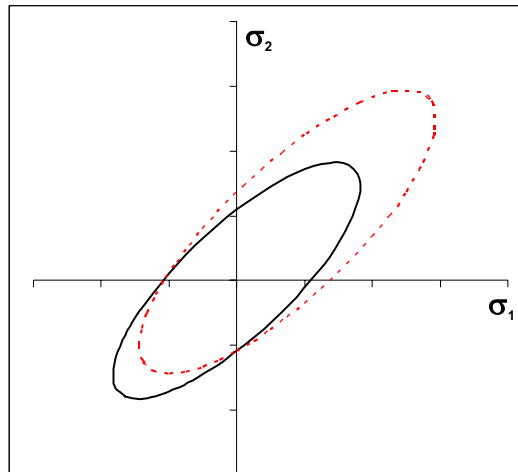


Fig. 3. The yield surface for J2 yield criterion with mixed-hardening

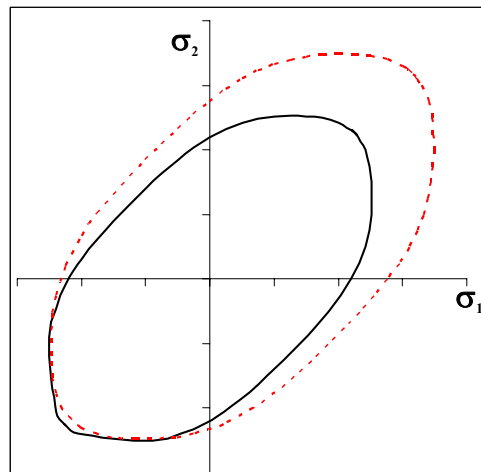


Fig. 4. The yield surface for Hosford's yield criterion with mixed-hardening

$$\begin{aligned} \omega_1 &= \sigma_I - r_I, & \omega_2 &= \sigma_{II} - r_{II}, \\ \omega_3 &= (\sigma_I - r_I) - (\sigma_{II} - r_{II}) \end{aligned} \tag{11}$$

where σ_I, σ_{II} are the principal stresses and r_I, r_{II} are the back stresses in principal stress directions.

In the constitutive law of the form (3), the incremental plane-stress moduli $\bar{L}^{\alpha\beta\kappa\gamma}$ using the flow theory are given by

$$\bar{L}^{\alpha\beta\kappa\gamma} = L^{\alpha\beta\kappa\gamma} - \frac{L^{\alpha\beta 33} L^{33\kappa\gamma}}{L^{3333}} \tag{12}$$

and

$$L^{ijkl} = L_{ijkl}^e - \frac{L_{ijrs}^e \mu_{rs} \mu_{pq} L_{pqkl}^e}{h + \mu_{tu} L_{tumn}^e \mu_{mn}} \quad (13)$$

where h is an instantaneous hardening ratio, μ_{ij} is the tensor of the yield surface normal and L_{ijkl}^e is the incremental modulus for elastic deformation, given by

$$L_{ijkl}^e = \frac{E}{1+\nu} \left[\frac{1}{2} (\delta_{ik} \delta_{jl} + \delta_{il} \delta_{jk}) + \frac{\nu}{1-2\nu} \delta_{ij} \delta_{kl} \right] \quad (14)$$

where E is Young's modulus, ν is Poisson's ratio and δ_{ij} is the Kronecker delta. The uniaxial stress-strain curve of the metal is modeled by a power-law hardening relation of the following form :

$$\frac{\sigma}{\sigma_y} = \begin{cases} \frac{E}{\sigma_y} \varepsilon & , \sigma \leq \sigma_y \\ \left(\frac{E}{\sigma_y} \varepsilon \right)^n & , \sigma > \sigma_y \end{cases} \quad (15)$$

where σ_y is the yield stress and n is a strain-hardening coefficient.

RESULTS AND DISCUSSION

To investigate the influence of back stresses for mixed-hardening materials (both isotropic and anisotropic metals) on the wrinkling formation in deep-drawing process, parametric study in terms of principal stresses has been carried out. The principal stresses in the cup wall in deep-drawing process shows in Fig. 5.

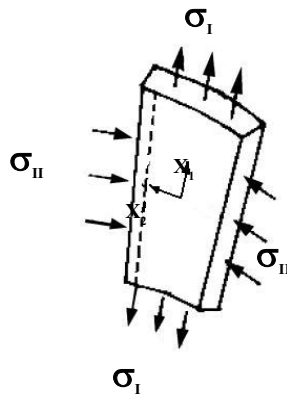


Fig. 5. The stress state in the cup wall in deep-drawing process

For the isotropic metal, the ratios of R_2 / R_1 and t / R_2 are fixed at constant values of 0.5 and 0.02 respectively, the material constants are taken as follows : $\nu = 0.3$, $E = 200$ GPa, $\sigma_y / E = 0.001$ and $n = 0.1$. This data are chosen according to Neale and Tugcu work.

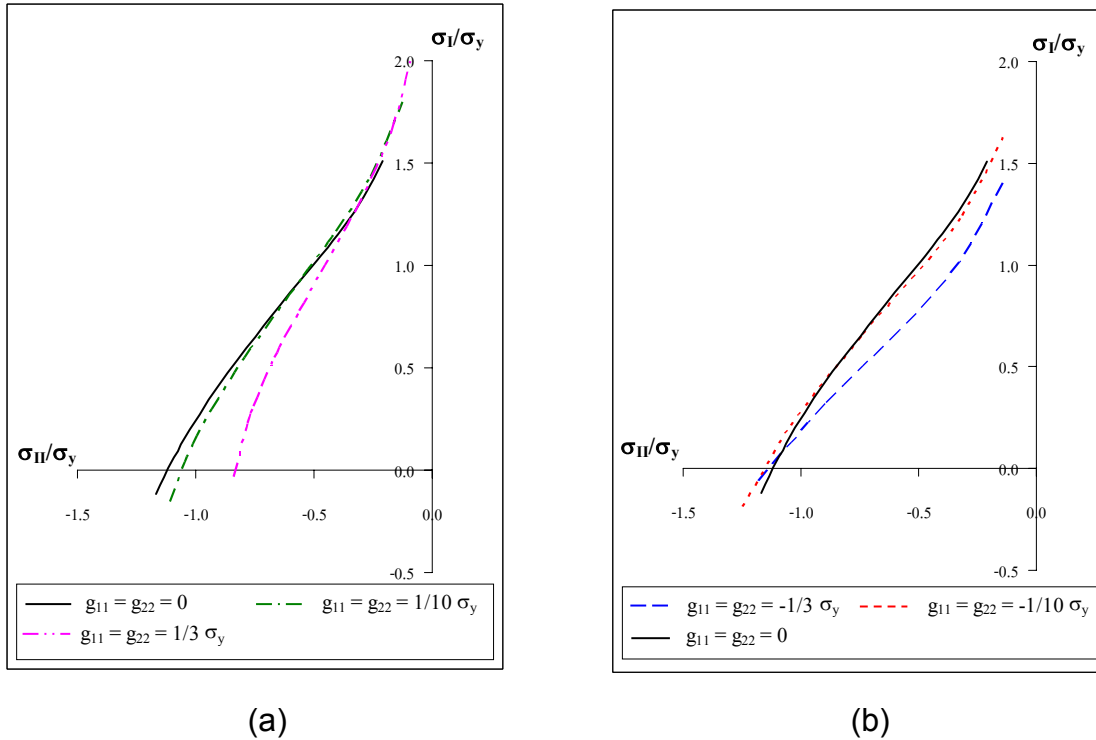


Fig. 6. The critical stress states for various deviatoric part of back stresses.

For the negative deviatoric back stresses with the same magnitude of back stress components (namely $g_{11} = g_{22}$), Fig. 6(a) shows that σ_{II} / σ_y changes insignificantly at σ_I / σ_y of about 0. However, σ_I / σ_y increases ($\sigma_I / \sigma_y > 0$) and σ_{II} / σ_y decreases when the magnitude of the deviatoric back stresses increase.

For the positive deviatoric back stresses, Fig. 6(b) shows that σ_{II} / σ_y changes insignificantly at $\sigma_I / \sigma_y > 1.2$. However, σ_I / σ_y decreases ($\sigma_I / \sigma_y < 1.2$) and σ_{II} / σ_y decreases when the magnitude of the deviatoric back stresses increase.

Fig. 7(a) shows the effects of back stress components g_{11} on the wrinkling limits. Increasing the back stress component g_{11} will increase the critical stresses. Fig. 7(b) shows the effects of back stress components g_{22} on the wrinkling limits. Increasing the back stress component g_{22} will decrease the critical stresses.

For the anisotropic metal, the ratios of R_2 / R_1 and t / R_2 are fixed at constant values of 0.5 and 0.02 respectively. In this study, the sheet thickness of 0.88 mm is used. The material constants, based on the mechanical properties of the CHSP35E material used by Kim and Son [4], are taken as follows : $\nu = 0.3$, $E = 200$ GPa, $\sigma_y = 220$ MPa, $\bar{R} = 1.36$ and $n = 0.19$.

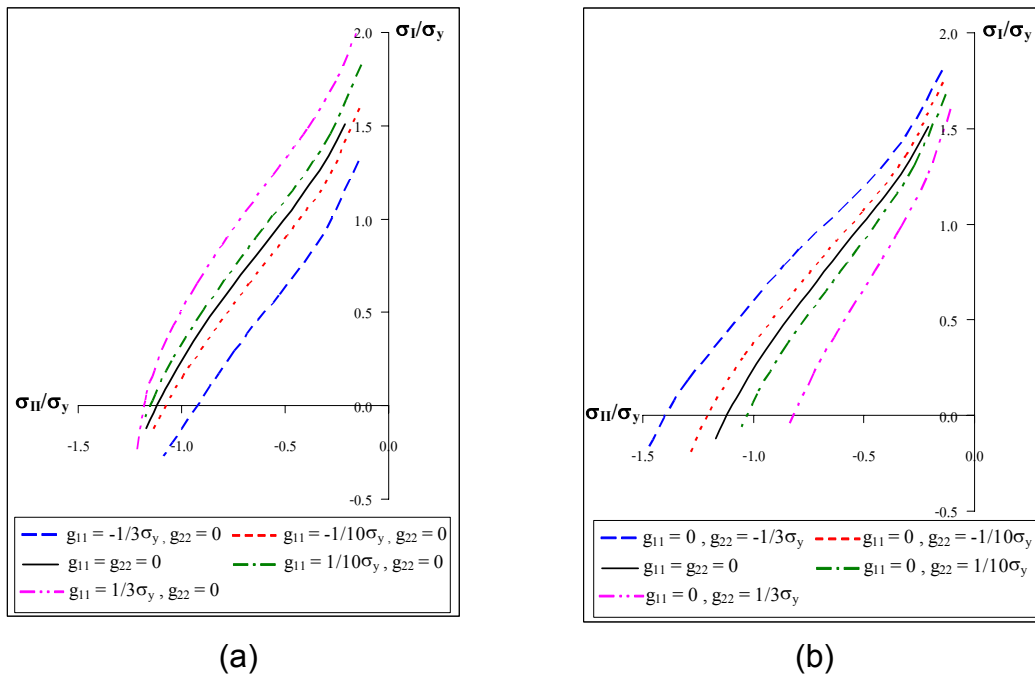


Fig. 7. The critical stress states for various deviatoric part of back stresses.

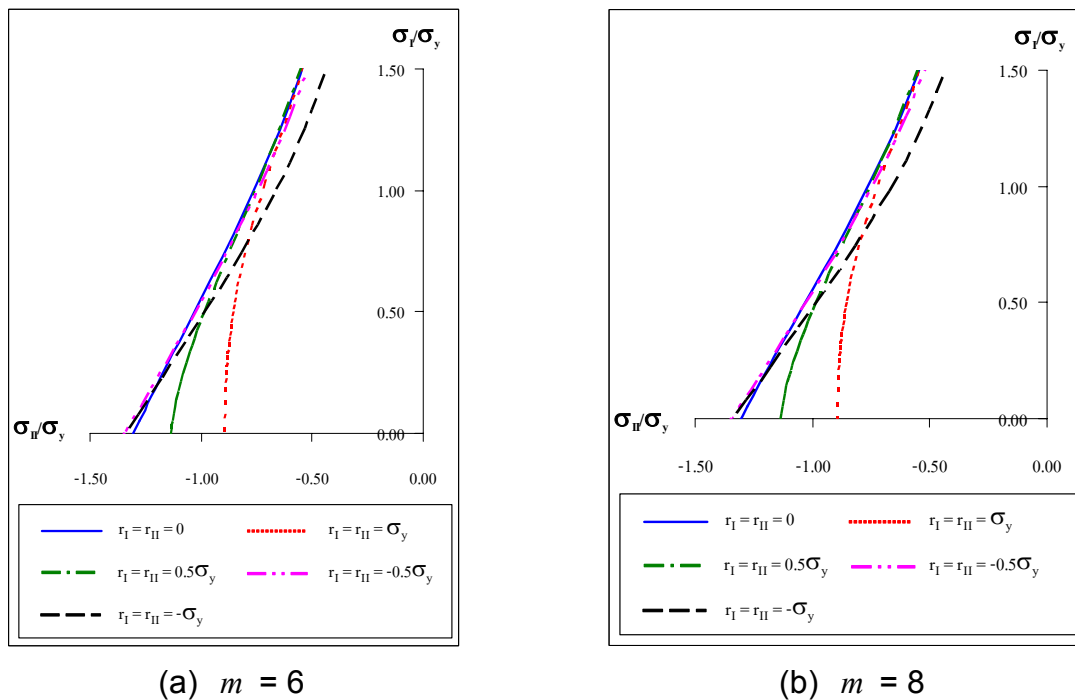


Fig. 8. The critical stress states for various back stresses

Fig. 8(a) and Fig. 8(b) show the effect of back stresses with $r_I = r_{II}$ on the wrinkling limit based on Hosford's yield criterion with $m = 6$ and 8 respectively. For the negative back stresses, σ_{II} / σ_y changes insignificantly at σ_I / σ_y of about 0. However, σ_I / σ_y increases ($\sigma_I / \sigma_y > 0$) and σ_{II} / σ_y decreases when the magnitude of the back stresses

increase. For the positive deviatoric back stresses, σ_{II}/σ_y changes insignificantly at $\sigma_I/\sigma_y > 1.2$. However, σ_I/σ_y decreases ($\sigma_I/\sigma_y < 1.2$) and σ_{II}/σ_y decreases when the magnitude of the back stresses increase.

Fig. 9(a) shows the effect of back stresses with $r_I = r_{II}$ on the wrinkling limit based on Hosford's yield criterion with $m = 6$ and 8. The critical stress ratios decrease as m increases. This is in agreement with the results of Kim and Son's work.

Fig. 9(b) shows the effect of back stresses with $r_I = r_{II}$ on the wrinkling limit based on Hosford's yield criterion with $n = 0.19$ and 0.22. The effect of the back stresses for the critical stresses is the same trend in Fig. 8(a) and Fig. 8(b). Furthermore, the critical stress ratio increase as n increases. This is in agreement with the results of Kim and Son's work.

Fig. 9(c) shows the effect of back stresses with $r_I = r_{II}$ on the wrinkling limit based on Hosford's yield criterion with $\sigma_y = 220$ and 270 MPa. The effect of the back stresses for the critical stresses is the same trend in Fig. 8(a) and Fig. 8(b). Furthermore, the critical stresses for the onset of wrinkling decrease as yield stress increases. This is in agreement with the results of Kim and Son's work.

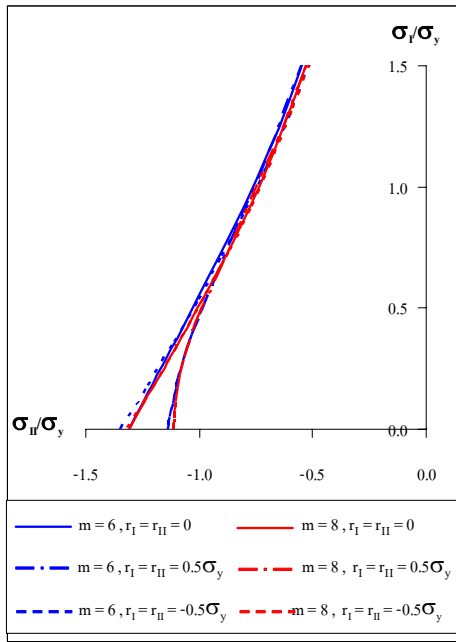
Fig. 9(d) shows the effect of back stresses with $r_I = r_{II}$ on the wrinkling limit based on Hosford's yield criterion with $\bar{R} = 1.36$ and 2. The effect of the back stresses for the critical stresses is the same trend in Fig. 8(a) and Fig. 8(b). Furthermore, the critical stress ratios for the onset of wrinkling change negligibly. This is in agreement with the results of Kim and Son's work.

CONCLUSION

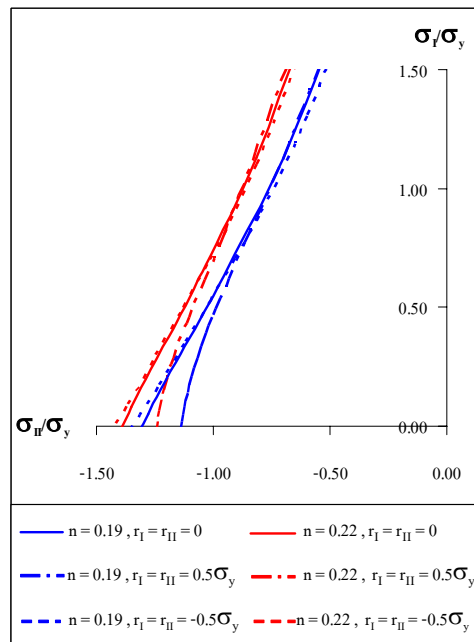
The analysis of critical principal stresses for the onset of wrinkle formation of mixed-hardening metal sheets has been performed to investigate the effects of back stresses on the wrinkling limit curves in deep-drawing processes.

Numerical results show for both isotropic and anisotropic materials that increasing back stress component in the direction of the principal axis X_I will increase the critical principal stresses. On the other hand, increasing back stress component in the direction of the principal axis X_{II} will decrease the critical principal stresses. In case of equal back stress components, increasing the positive back stress components will decrease the critical stress σ_{II} . On the other hand, decreasing the negative back stress components will decrease the critical stress σ_{II} .

For the anisotropic material, the effects of material constants m , n , σ_y and \bar{R} were examined. As the numerical results, increasing the yield function exponent m will decrease the positive critical stress ratios. Increasing the hardening coefficient n will increase the critical stress ratios. The critical principal stress ratios decrease as the yield stresses increase. Increasing anisotropy parameter \bar{R} will increase the positive critical principal stress ratios but decrease the negative critical principal stress ratios.

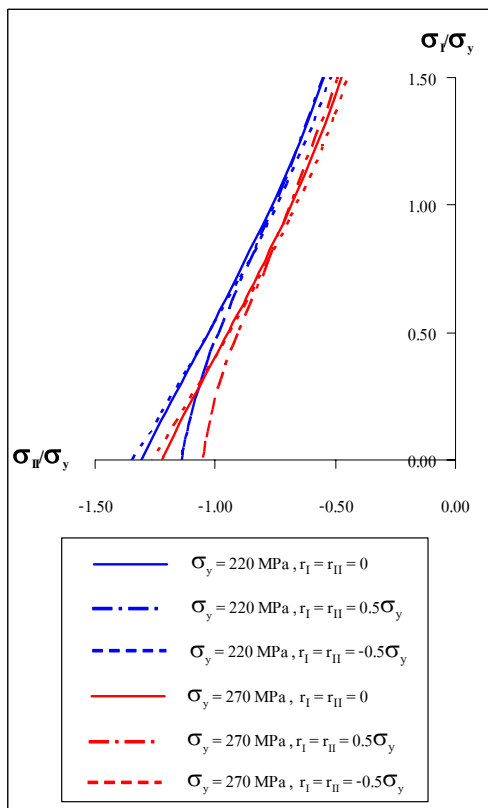


(a) $m = 6$ and 8

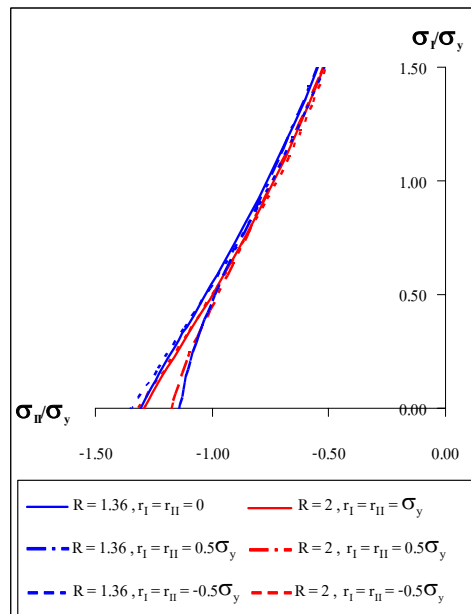


(b) $n = 0.19$ and 0.22

Fig. 9. The critical stress states for various back stresses



(c) $\sigma_y = 220$ and 270 MPa



(d) $\bar{R} = 1.36$ and 2

Fig. 9. The critical stress states for various back stresses

REFERENCES

- [1] Hutchinson, J.W., "Plastic buckling", *Advanced in Applied Mechanics*, 14, pp 67-144, (1974).
- [2] Hutchinson, J.W. and Neale, K.W., "Wrinkling of curved thin sheet metal", In J. Salecon, editor. *Plastic instability. Presses Ponts et Chaussees*, pp 71-78, (1985).
- [3] Neale, K.W. and Tugcu, P., "A numerical analysis of wrinkle formation tendencies in sheet metals", *International Journal for Numerical Methods in Engineering*, 30, pp 1595-1608, (1990).
- [4] Kim, Y.S. and Son, Y.J., "Study on wrinkling limit diagram of anisotropic sheet metals", *Journal of Materials Processing Technology*, 97, pp 88-94, (2000).
- [5] Hosford, W.F., "On yield loci of anisotropic cubic metals", *Seventh North Am. Metalworking Res. Conf.*, 191-196, (1979).
- [6] Tugcu, P., Neale, K.W., Wu, P.D. and MacEwen, S.R., "Effect of planar anisotropy on wrinkle formation tendencies in curved sheets", *International Journal of Mechanical Sciences*, 43, pp 2883-2897, (2001).
- [7] Barlat, F., Lege, D.J. and Brem, J.C., "A six-component yield function for anisotropic materials", *International Journal of Plasticity*, 7, pp 693-712, (1991).
- [8] Karafillis, A.P. and Boyce, M.C., "A general anisotropic yield criterion using bounds and a transformation weighting tensor", *Journal of the Mechanics Sciences*, 41, pp 1859-1886, (1993).
- [9] De Magalhaes Correia, J.P. and Ferron G., "Wrinkling predictions in the deep-drawing process of anisotropic metal sheets", *Journal of Materials Processing Technology*, 128, pp 178-190, (2002).
- [10] De Magalhaes Correia, J.P. and Ferron G., "Analytical and numerical investigation of wrinkling for deep-drawn anisotropic metal sheets", *International Journal of Mechanical Sciences*, 45, pp 1167-1180, (2003).
- [11] De Magalhaes Correia, J.P. and Ferron G., "Wrinkling of anisotropic metal sheets under deep-drawing: analytical and numerical study", *Journal of Materials Processing Technology*, 155-156, pp 1604-1610, (2002).
- [12] Ferron, G., Makkouk, R. and Morreale, J., "A parametric description of orthotropic plasticity in metal sheets", *International Journal of Plasticity*, 10, pp 431-449, (1994).